Journal of Hazardous Materials 205–206 (2012) 189–197

Contents lists available at SciVerse ScienceDirect

Journal of Hazardous Materials

journal homepage: www.elsevier.com/locate/jhazmat

Volatility and mixing states of ultrafine particles from biomass burning

A.M.M. Maruf Hossain, Seungho Park, Jae-Seok Kim, Kihong Park*

School of Environmental Science & Engineering, Gwangju Institute of Science & Technology, Gwangju, Republic of Korea

ARTICLE INFO

Article history:
Received 21 June 2011
Received in revised form
16 December 2011
Accepted 21 December 2011
Available online 29 December 2011

Keywords:
Biomass burning
Ultrafine particles
VTDMA (volatility tandem differential mobility analyzer)
Organic carbon
Black carbon

ABSTRACT

Fine and ultrafine carbonaceous aerosols produced from burning biomasses hold enormous importance in terms of assessing radiation balance and public health hazards. As such, volatility and mixing states of size-selected ultrafine particles (UFP) emitted from rice straw, oak, and pine burning were investigated by using volatility tandem differential mobility analyzer (VTDMA) technique in this study. Rice straw combustion produced unimodal size distributions of emitted aerosols, while bimodal size distributions from combustions of oak (hardwood) and pine (softwood) were obtained. A nearness of flue gas temperatures and a lower CO ratio of flaming combustion (FC) to smoldering combustion (SC) were characteristic differences found between softwood and hardwood. SC emitted larger mode particles in higher numbers than smaller mode particles, while the converse was true for FC. Rice straw open burning UFPs exhibited a volatilization behavior similar to that between FC and SC. In addition, internal mixing states were observed for size-selected UFPs in all biomasses for all combustion conditions, while external mixing states were only observed for rice straw combustion. Results for FC and open burning suggested there was an internal mixing of volatile organic carbon (OC) and non-volatile core (e.g., black carbon (BC)), while the SC in rice straw produced UFPs devoid of non-volatile core. Also, it was found that volatility of constituting OC in FC and SC particles was different.

1. Introduction

Atmospheric aerosols may seem insignificant, yet they have a potentially huge impact, ranging from off-setting global warming [1] to potentially modifying climate systems as well as stimulating research for enhancement of their positive roles in mitigating climate change. In particular, fine and ultrafine aerosols in the atmosphere have been strongly correlated to adverse health effects, though their causative relations or mechanisms are not well understood [2]. To this end, biomass burning in agricultural fields and forest fire events, and residential biomass burning are significant contributors to atmospheric aerosol loads. Carbonaceous aerosols, largely emitted from such biomass burning, account for a large fraction of air particulate matter [3–7]. The organic carbon (OC) and black carbon (BC) aerosols, comprising the pool of carbonaceous aerosols, are produced due to incomplete combustion from various fuels [8]. For example, in the urban atmosphere of Los Angeles it was found that approximately 40% of the total fine particulate mass loading could be accounted for as being carbonaceous aerosols [9–12].

In recent years, a growing number of studies have tried to address the particulate matter emitted from biomass burning in different ways (e.g., with lab-scale simulations of field burning, fireplace combustion, wood-stove burning, and energy producing boilers) [13–24]. The size distributions, further differentiated into different burning conditions, are important for determining which particle sizes are likely to be added in what abundance into the atmosphere and undergo different processes therein, the most important of which would be to determine their interactions based on radiative forcing and public health consequences. Previous studies have shed some light on the size distribution of particles emitted from the burning of some of these biomasses, as well as on their chemical compositions [13–16]. Petters et al. [25] determined hygroscopicity and cloud condensation nuclei (CCN) activity for particles (30–300 nm) emitted by open burning of various biomass fuels. However, there has been limited information on the size distributions of those emitted from biomass burning for the whole diameter range (20 nm–10 μm), which could provide better insight into the emission characteristics of these particles. Similarly, there has been limited information on the volatility and mixing state of size-selected ultrafine particles emitted from biomass burning obtained by simulating different burning conditions in laboratory scale. Ultrafine particles may have a higher reactivity or toxicity due to their higher surface area-to-volume ratio compared to coarse particles, thereby strongly affecting human health [26,27]. Indeed, the existence of volatile carbonaceous species such as PAH and non-volatile BC could provide a useful insight into their effects on human health. Also, the volatility measurements of ultrafine particles could

* Corresponding author. Tel.: +82 062 715 3279.
E-mail address: kpark@gist.ac.kr (K. Park).

0304-3894/$ – see front matter © 2011 Elsevier B.V. All rights reserved.
doi:10.1016/j.jhazmat.2011.12.061

be an alternative means to study general chemical characteristics of carbonaceous species. For instance, it was reported that interaction of particles with incoming solar light was significantly affected by their mixing state, affecting the earth's radiation balance [1]. As such, adequate information on the volatility of biomass combustion emitted aerosols as well as their mixing states is likely to take on further significance, especially when the carbonaceous aerosols from biomass burning (mainly comprised in BC and OC) being reported as one of the most significant groups for potential implications, both in terms of forcing estimates [3,7,28–32] as well as public health consequences [33–36].

In this study, burning events in agricultural fields and during forest fires were simulated in a laboratory. Oak (hardwood) and pine (hardwood) as well as rice straw, which is known to be one of the most widely grown cereal crops in Korea or East Asia countries, were used as fuels. We examined number size distribution, volatile properties, existence of non-volatile core, and mixing state of ultrafine particles burned from such biomasses with different burning conditions (flaming, smoldering, and open burning condition), based on scanning mobility particle sizer (SMPS), particle size distribution analyzer (PSD), and volatility tandem differential mobility analyzer (VTDMA) technique [37], along with a supplementary analysis of transmission electron microscopy/energy dispersive spectroscopy (TEM/EDS) data. The VTDMA measurement will provide useful insights into internal or external mixing state of size-selected ultrafine particles by heating and subsequently evaporating portions of the particles, and by examining the behavior of particle size change as a function of temperature.

2. Experimental

2.1. Fuels

Rice straw (*Oryza sativa*, 10.8% moisture), along with oak (10.6% moisture) and pine (11.2% moisture) were used as biomasses. Rice straw is a major material frequently included in the burning of agricultural fields in Korea or East Asia countries, while oak and pine are abundant in Korean forests and are often involved in forest fire events. The moisture contents were experimentally determined by using an oven-dying method (ASTM E1358). The rice straw was collected from a rural field outside Gwangju (Republic of Korea), while oak and pine samples were collected from a forest area near Yeosu, Republic of Korea. The two types of wood were selected as a representative hardwood (oak) and softwood (pine) in these forests, allowing us to project the general characteristics over other similar wood types.

2.2. Combustion system for simulating burning and sampling

A commercial combustion stove consisting of a 55 cm diameter, 80 cm tall vertical chimney was used to simulate the burning conditions (Fig. 1A). The air intake for the combustion air was located at the bottom of the combustion chamber. The chimney was connected to a 35 cm diameter by 40 cm tall cylindrical dilution chamber, providing ~25-fold HEPA-filtered dilution air by using a mixing fan installed at the bottom of the chamber to dilute the air before it enters the measurement instruments. A sampling probe was placed at a 1 m height inside the chimney. An isokinetic sampling was ensured by placing the sampling tube in different positions and thereby measuring the two flows (one at the end of chimney, and the other at the end of sampling tube coming from inside the chimney). The appropriate alignment of the sampling tube was conducted in order to represent isokinetic sampling from the chimney. The flow rates in the dilution chamber were controlled by a mass flow controller. Previously, due to the distributed presence of aromatic compounds in the gas and aerosol phases from the source emissions, whose partition is dependent on the temperature of the system as well as partial pressures of the compounds in gas phase, Hildemann [38] developed a dilution stack sampler for simulating ambient conditions after emission, in order to collect organic aerosols. A similar dilution chamber was constructed in this study. Other flue gas characteristics (CO and CO_2 emissions with Unigas 4000+ Eurotron gas analyzer, and temperature with a K-type thermocouple) were measured at a 1 m height inside the chimney (the gas sampling line was not cooled before it entered the gas analyzers). The flue gas temperature was monitored at 1 m height of the chimney which is an integral part of the combustion system. Aerosol Measurements were conducted at 10 m away from the combustion facility, and the temperature measured at the entrance to the VTDMA system was almost similar to the ambient temperature (i.e., the residence time through the flow tube appears to be sufficient to allow the temperature of the flow to

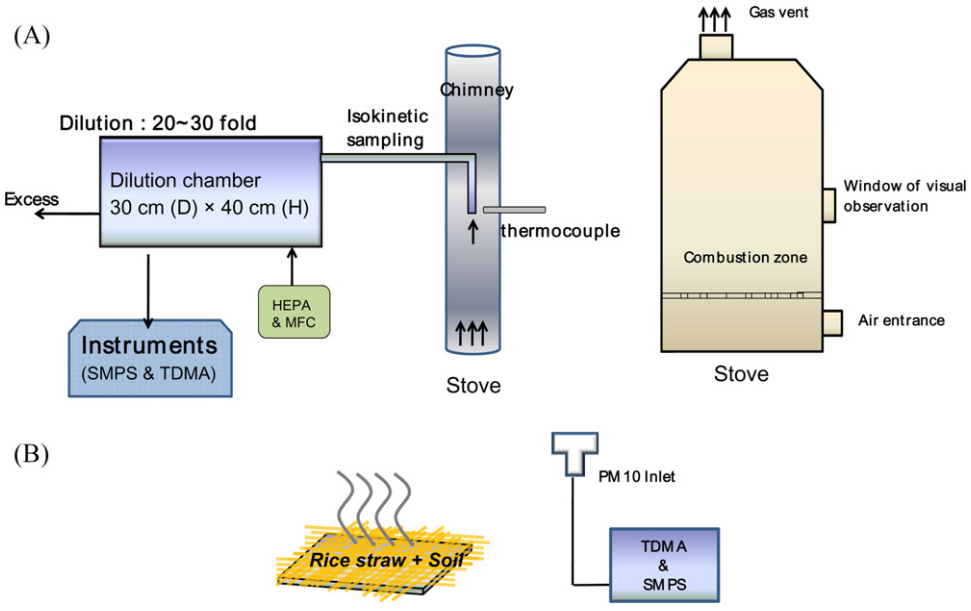

Fig. 1. Schematic of combustion system: (A) flaming and smoldering combustions and (B) open burning.

come to ambient level). The water vapor from the exhaust stream was removed by using two-column silica gel bed before entering into measurement instruments.

Flaming, smoldering, and open burning conditions were simulated in this study. At the bottom of the chamber there is an air intake vent, which could be closed or kept open. In flaming combustion experiment, the vent was kept open so that air could enter from beneath, whereas in the smoldering combustion experiment the air flow was obstructed. The flaming combustion was proceeded with visible flame, while no flame was seen during the smoldering combustion experiment. In unaided visual observations, flaming combustion yielded a dense stream of black particles, whereas the smoldering combustion produced a thick flow of white fumes. The smoldering combustion condition was produced by restricting the combustion air supply and overloading the firebox with fuel; vice versa for the flaming combustions. Previously, Tissari et al. [20] used these combustion conditions, although they used the term "normal" combustion instead of "flaming". An additional open field burning condition (outside of the combustion chamber) was simulated for rice straw by placing soil underneath the straw (Fig. 1B). The ambient conditions that prevail during real-world burning were left uncontrolled, except to the extent that the normal air entrance was obstructed in order to produce a smoldering condition which takes place in the absence of air renewal. Since the dilution ratio should be much larger for the open burning condition, it was suggested that some particles would be volatilized prior to measurement by the VTDMA system [39]. Indeed, this would be the case during real-world open-field burning. Here, a PM_{10} inlet was used to collect emissions during open burning and route them to the measurement instruments.

2.3. Measurement instruments

The particle size distributions were measured using a SMPS (TSI 3081 DMA and TSI 3022A CPC) for the range from 20 nm to 600 nm, whereas a PSD (TSI 3603) was used for 200 nm to 10 μm particles. In principle, the SMPS measures the mobility equivalent diameter while the PSD measures the aerodynamic equivalent diameter. In order to plot both measurements in a continuous plot, the aerodynamic equivalent diameters were converted to mobility equivalent diameters by assuming particle density information (from SMPS and PSD, the particle density was changed to have a consistent size distribution in the overlapping size range) by utilizing the equation "$d_{aero} = d_{mobility}\sqrt{(\rho_p/\rho_o)}$" where d_{aero}, $d_{mobility}$, ρ_p, and ρ_o are aerodynamic diameter, mobility diameter, particle density, and unit density (1 g/cm^3), respectively.

Volatility analyses of the emitted particles were performed using a VTDMA system. The VTDMA system consisted of two nano-DMAs (TSI 3085), two long-DMAs (to cover a wide size range), a heating tube, and one ultrafine condensation particle counter (UCPC) (TSI 3776) as shown in Fig. SI-1 (Supporting Information). The working principle of the VTDMA system used in this study and the basic method of calculating the volume fraction of volatile species was published previously [37]. Within the ultrafine size range, we selected particles of certain sizes by the first DMA, and the selected particles were exposed to increased temperature in a heated tube, and the subsequent particle size change was determined by the second DMA and UCPC. Note that SI-1 (Supporting Information) contains other considerations followed in explaining the volatility data in addition to defining the mixing states and error analyses used therein.

As (i) the sample was not an ambient atmospheric aerosol, but rather biomass combustion-emitted particles under isokinetic sampling, (ii) sampling was done in a closed system while maintaining specific burning conditions, and (iii) sampling was conducted under the condition of forced air supply; particle loss due to gravity or diffusion were not taken into consideration. Moreover, loss due to thermophoresis was not considered as there was no heating of the generated aerosols in the sampling stream. In the volatility analysis, additional heating of the size-selected particles could possibly cause error in measurement due to recondensation or nucleation of the volatile species evaporated from particles, in the cooling section of VTDMA system (as presented in case of thermodenuder in Saleh et al. [40]); however, Park et al. [37] have shown such error to be negligible for the VTDMA system used here. In the present study, the volatility of samples was measured over a relatively modest range of temperatures (20–250 °C). And though complete volatilization of organic material requires a 590 °C temperature under a nitrogen atmosphere and heating at 650 °C under an oxygen atmosphere is required to separate the non-volatile elemental carbon [41], we limited our experimentation to 250 °C. The remaining volume beyond 250 °C heating would not contain any volatile OC, leaving only the non-volatile core particles; this temperature is thus sufficient for separating volatile OC, and non-volatile OC and/or BC. The samples were also analyzed via TEM (JEOL JEM-2100F) and EDS (OXFORD INCAx-sight) to obtain morphological and elemental composition data, respectively.

3. Results and discussion

3.1. Size distributions

A summary of the burning conditions (flue gas temperature, CO ratio) and emitted particle mode diameters is listed in Table 1. In previous experiments, Tissari et al. [20] reported a flue gas temperature difference between normal (flaming) combustion and smoldering combustion (>200 °C and <200 °C, respectively, from data presented therein). They also reported elevated CO emissions during smoldering combustion (3.5 times of that of flaming combustion), which is consistent with the measured flue gas temperatures and CO emission ratios presented in the table. Hays et al. [14] reported varying CO/CO_2 trends between the flaming and smoldering combustion conditions as well as between different fuels. And Tissari et al. [19] described the influences of different factors, such as insufficient air supply (in flaming combustion) and low diffusion rate of oxygen and cooling of combustion chamber (in smoldering combustion), causing incomplete combustion and thereby limiting CO_2 emissions. However, differences in biomass densities would utilize the available oxygen differently, and thus different CO/CO_2 ratios can be found in a single burning condition-some of which may conform to values of other burning conditions. In that regard, descriptions in terms of CO ratio would be a more reliable measure for characterizing different burning conditions, which is consistent in all our observations. Moreover, it is also seen in Table 1 that when the flue gas temperature gap between flaming and smoldering conditions is narrow (in the case of wood), the CO ratio between the conditions is also low, and vice versa. Hence, this can be another characteristic for defining different burning conditions.

The size distributions of particles from rice straw burning (20 nm–10 μm diameter range) at three different burning conditions are presented in Fig. 2. All combustion conditions resulted in unimodal particle-size distributions, which is similar to the results reported by Hays et al. [14] which show unimodal size distributions for almost all combustion experiments, though they were for another cereal crop (wheat straw, not rice straw) as well as for a limited size range (10–400 nm). For rice straw, a shift of the mode diameter in the positive direction is evident from Table 1, in the order of open burning (53.3 nm) < smoldering combustion (88.2 nm) < flaming combustion (140.7 nm) conditions. One reason for this rank order might be due to particle size alteration by the

Table 1
Summary of burning conditions and mode diameters of particles obtained from burned biomasses.

Biomass	Combustion condition	Flue gas temp.	CO ratio of the flaming to smoldering	Mode diameters (nm)
Rice straw	Flaming	227 °C	1:2.6	140.7
	Smoldering	193 °C		88.2
	Open burning	⋘193 °C	–	53.3
Oak (hardwood)	Flaming	236 °C	1:2.4	121.9, 488.5
	Smoldering	165 °C		145.9, 569.6
Pine (softwood)	Flaming	213 °C	1:1.8	140.7, 587.5
	Smoldering	199 °C		174.7, 645.8

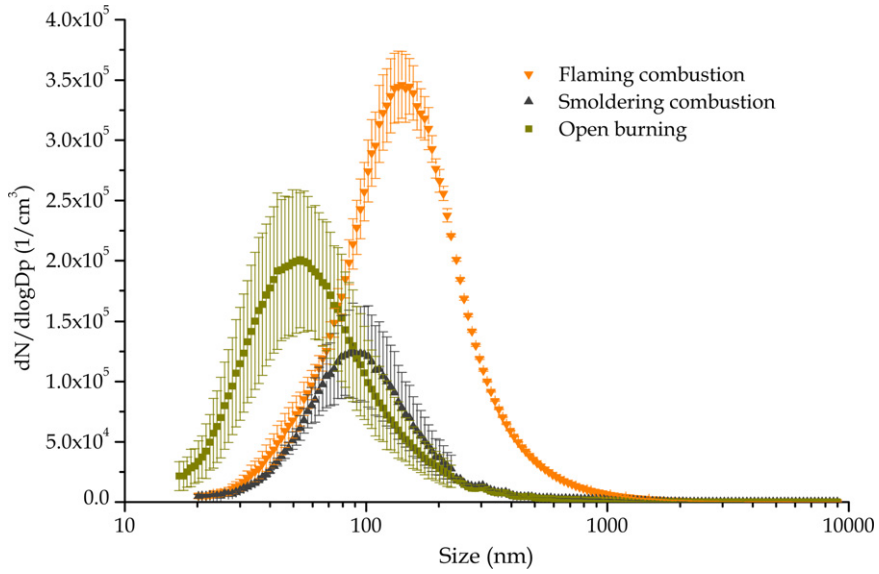

Fig. 2. Size distributions of particles from rice straw burning at different conditions.

diverse OC compounds, as they are affected by differential temperatures in the vicinity of burning at different burning conditions. For example, Hays et al. [14] reported on the OC fraction in burning rice straw, which was comprised of more than 200 compounds with a significant portion unresolved. These detected compounds were found to have melting points well distributed over a temperature range of less than 0 °C to more than 250 °C. Therefore, the differential flue gas temperatures under different burning conditions may act differently for the various particles melting points, potentially easing the process of attachment with other particles, resulting in an increased mode diameter. It was reported that the low combustion efficiency in the slow burning of agricultural residues due to underlying top soil produced larger particles compared to faster burning (Kleeman et al. [42]). Also, different dilution ratios and sampling temperature can affect gas-to-particle partitioning, leading to differences in size distribution (Lipsky and Robinson [43]). In this study, the order of mode diameters was found to be the same as the order of increase in flue gas temperature, as presented in Table 1 (no definitive temperature value was mentioned for open burning flue gas temperature due to its non-standard nature, though it was well-below of the flue gas temperature of smoldering combustion). During the open burning of rice straw, depending on the unburned fuel remaining, fuel load, and wind characteristics, the burning resembles both partly flaming and partly smoldering conditions. In open burning and smoldering combustion conditions, the modes were in the ultrafine range (<100 nm), then shifted into the fine range (0.1–2.5 μm) for the flaming condition.

In Table 1, the CO emission ratio between the flaming and smoldering conditions and flue gas temperature difference for the two combustion conditions also correlate to the hardness of the two types of woods (i.e., they has a different vulnerability to burning under similar conditions). Nearness in the observed flue gas temperatures of the two combustion conditions (only a 14 °C gap between flaming and smoldering combustions) and a lower CO ratio (1:1.8) were observed in softwood (pine). However, in case of oak (hardwood), these burning condition differences are sharper, accompanied by more contrasting flue gas temperatures (71 °C gap between flaming and smoldering combustions) and higher CO emission ratio (1:2.4). The nature of the woods can also be explained in that connection; being more vulnerable to burning, softwood would demonstrate a lower contrast between burning conditions (lower CO ratio and narrower flue gas temperature gap between flaming and smoldering conditions). Such distinctions also conform to the regularity observed in mode diameter shift (mode diameters in softwood flaming combustion are higher than the mode diameters for hardwood, and similar in cases of smoldering combustion). Therefore, in terms of the woods' vulnerability to burning, the wood more vulnerable to burning (softwood) would result in larger mode diameters than from wood less vulnerable to burning (hardwood).

Size distributions of particles emitted from oak and pine combustion (20 nm–10 μm diameter range) for flaming and smoldering conditions are presented in Fig. 3A and B, respectively. For both types of the woods, the bimodal size distributions were obtained in both flaming and smoldering combustion conditions. Previously, Kleeman et al. [15] presented oak and pine size distributions within a diameter range from 20 nm to 3 μm through combined measurements obtained by the SMPS and optical particle counter (OPC) (fireplace burning; with no distinction between different burning conditions); however, the end result was a single mode in

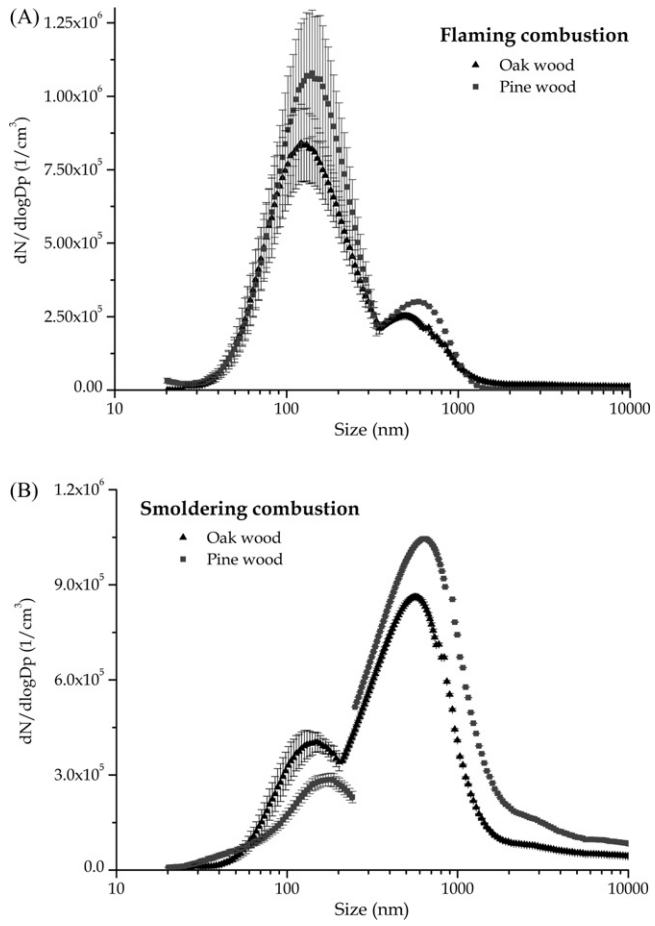

Fig. 3. Size distributions of particles from oak and pine for (A) flaming combustion and (B) smoldering combustion.

each distribution near a particle diameter of 200 nm. For the combustion of different types of wood, Wardoyo et al. [21] concluded that number emissions were lower, though there were higher PM mass concentrations for slow burning (smoldering combustion) versus fast burning (flaming combustion). Such a conclusion could be arrived at as the size distributions resulted in only one mode in all cases due to the limited measured size range under their study (13–600 nm, obtained by the SMPS). However, for an extended size range, as in this study, differing burning inter-comparisons between multiple modes are shown, which does not allow for such a straightforward conclusion. In our study, the flaming condition resulted in higher particle numbers at the smaller mode diameter, and lower particle numbers at the larger mode diameter, with the converse being true for the smoldering combustion condition.

From Fig. 3B, it is clear that smoldering combustion led to the emission of larger particles (e.g., tar balls) in comparatively much higher numbers than for the smaller sized particles, which can be due to the condensation of organic species [17]. On the other hand, flaming combustion may have led to the emission of more BC or soot-like particles that are smaller in diameter (Fig. 3A). In the case of rice straw (Fig. 2) such a distinction could not be made due to the unimodal nature of the distributions. It should be noted here that the particle number concentrations for different fuels should not be used to compare among the fuels in a quantitative manner, as they are not directly related to the quantification of burned fuel amount (e.g., number emission factor). The purpose of comparing size distributions is only to show the distribution tendency over the given size range. From this perspective, the emitted particle size distributions of oak and pine exhibit similar tendencies (bimodal, whereas the mode diameters of emitted particles increased from hardwood/oak to softwood/pine combustion) that sharply contrast that of rice straw combustion, which exhibited unimodal particle size distributions in all three burning conditions.

One hypothesis is that such general behavior can be correlated with the nature of the biomasses. As oak and pine woods are consolidated masses, whereas rice straw is a void mass with a porous structure, rice straw could be subject to more uniform and efficient burning-which would thereby result in the observed unimodal particle size distributions. In contrast, the consolidated mass in wood would be subject to burning from the outer to inner layers of a log within a single set of burning condition, thereby resulting in more than one mode in the particle size distribution. It should also be noted that the time resolution of SMPS did not capture any particular time dependence in the mode/modality of the size distributions. Rather, every log contains numerous circular layers with each layer typically indicating one year of the tree's growth; depending on the age of each tree, the number of interior layers would vary. Such layering might also cause more than one mode in their size distribution in contrast to the simple structure of rice straw, which results in only single modes for all burning conditions.

3.2. Volatility and mixing states of the biomass burning ultrafine particles

The carbonaceous nature of biomass burning aerosols and the dependence of the relative abundance of OC and BC components on the alteration of burning conditions are becoming evident from a growing number of studies [13–15,18,20]. This body of literature recommends a higher temperature firing combustion, which results in a significant amount of refractory BC, whereas lower temperature combustion yields particles with a lot of OC. In this study, flaming combustion resembled such higher temperature firing combustion, and smoldering combustion resembled lower temperature smoldering combustion. The EDS data in Figs. SI-2–4 (Supporting Information) also reveal a high carbon peak followed by oxygen giving evidence as to carbonaceous nature of such particles. Therefore, instead of repeating efforts in establishing these well-known results in our burning simulations, we used these results to further our understanding.

Figs. 4 and 5 presents the volatility of 47–116 nm particles obtained from rice straw, oak, and pine for different burning conditions (flaming combustion = FC, smoldering combustion = SC, open burning = 'open'). The slopes of each line in Figs. 4 and 5 indicate the existence of varying volatile compounds, i.e., internal mixing states. In Fig. 4, with the exception of 116 nm particles during flaming combustion, all other size-selected particles exhibited more than one trend line upon volatilization (i.e., they were externally mixed). However, no external mixing states were observed for the oak and pine combustion-emitted particles (Fig. 5). In Fig. 4, for the 49 nm FC particles up to 70 °C heating, the 47 nm SC particles up to 50 °C heating, the 106 nm SC particles up to 70 °C heating, and for the 104 nm open burning particles up to 50 °C heating, no branching of lines was observed. Only from those points onward did the divergence occur, thereby differentiating two types of particles. Similar branching also occurred for data points at higher heating temperatures, suggesting that multiple types of particles were externally mixed for the given size-selected particles.

In Fig. 5, unlike the rice straw smoldering combustion-emitted particles, the smoldering combustion-emitted particles from both oak and pine contained non-volatile cores (i.e., not completely volatilized at 250 °C, very small cores remained). Data suggest that wood burning produced a significant amount of ultrafine particles having non-volatile core (BC) that later included OC on their surfaces. Again, apart from the observed lower flue gas temperatures of smoldering combustion than for flaming combustion

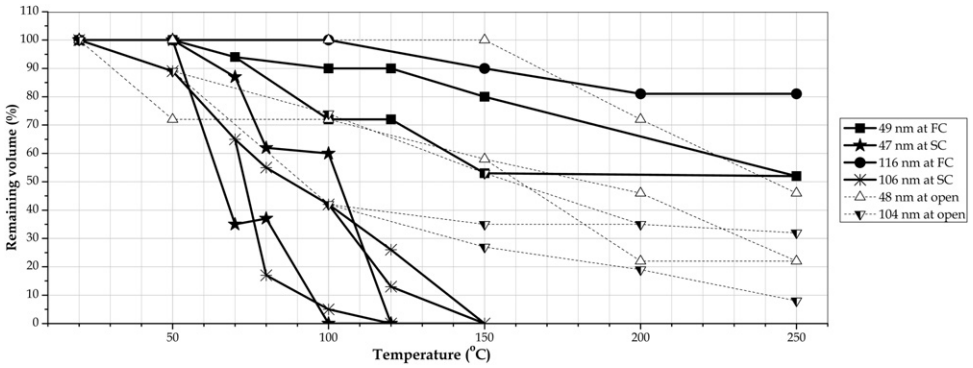

Fig. 4. Remaining volume fractions of size-selected particles (47–116 nm) from rice straw combustion as a function of heater temperature.

in wood, the reason for smoldering combustion-emitted ultrafine particles exhibiting a much higher volatility than flaming combustion-emitted ultrafine particles would largely be due to the composition of the particles. This difference implies that the smoldering combustion-emitted particles have a higher fraction of volatile species than the flaming combustion-emitted particles. This consideration supports the larger OC-nature of smoldering combustion-emitted ultrafine particles, whereas the larger BC- and/or non-volatile OC nature is evident in flaming combustion-emitted ultrafine particles. Fine et al. [13] reported around a 7-times higher OC generation than EC from a fireplace combustion experiment with pine (with no distinction between different burning conditions), while the majority of the OC fraction was comprised of unknown organics. Kleeman et al. [15] also showed that the compositional distribution of PM emissions from fireplace burning of oak and pine, were mostly comprised of OC, with minor EC fractions. Indeed, in other studies associated with wood burning in fireplaces or wood-stoves, results produced for different types of woods correspond to the volatility characteristics of oak and pine wood burning particles shown here. For instance, Rau [18] reported

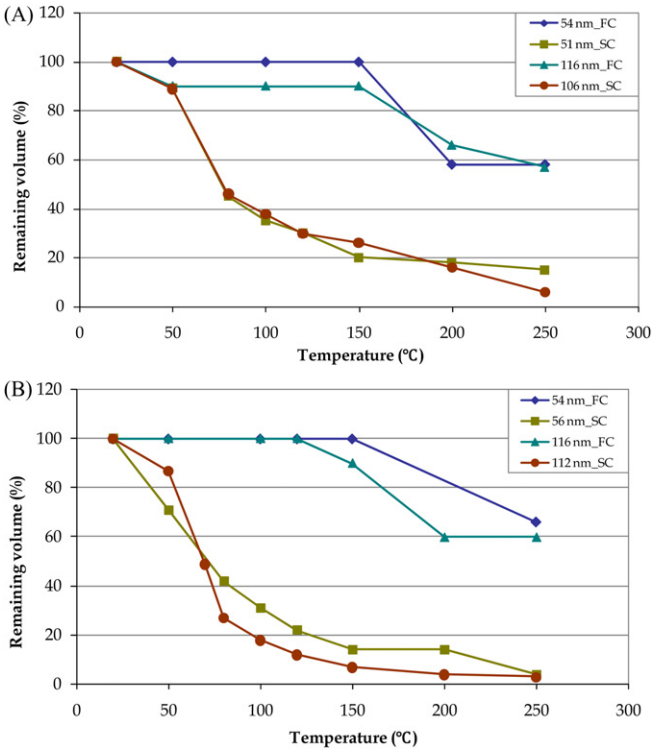

Fig. 5. Volatility of particles from (A) oak and (B) pine combustion.

on OC contribution to the total particle mass for a woodstove to be 14% for burning conditions with a surplus air supply (i.e., flaming combustion), while the OC contribution was as high as 57% under conditions with restricted air supply conditions (i.e., smoldering combustion). Tissari et al. [20] reported the presence of 67–69% particulate organic matter, with only 22–27% EC, in smoldering wood combustion; whereas there was only 33% particulate organic matter and 32% EC in normal (flaming) wood combustion. They also interpreted the larger particle size, higher effective density, and closed structure of particles in smoldering combustion as being due to organic matter condensation on the agglomerated soot particles. Carrico et al. [44] also reported that fuels burned in a smoldering condition produced aerosols with a large OC mass fraction.

As shown in Figs. 4 and 5, except for limited volatilization (<20%) of the 50 nm rice straw combustion-emitted particles and 100 nm oak combustion-emitted particles, all other flaming combustion-emitted particles underwent no volatilization up to 100 °C. In contrast, all smoldering combustion-emitted particles underwent major volatilization (>60%) within 100 °C, thereby indicating that the original OC in the flaming and smoldering combustion-emitted ultrafine particles are also different. Our data suggest that the VTDMA technique could be useful to differentiate mixture of compounds having different volatility.

The observed mixing states in rice straw combustion-emitted ultrafine particles (multiple lines in volatility curve in Fig. 4) can be interpreted by the diverse volatile OC compounds present in such particles [14], having distributed melting and boiling points over the temperature range as observed from our library search, in contrast to any BC fraction of these particles. In our library search, many of the 216 OC compounds that Hays et al. [14] reported to be present in rice straw during open burning, as per gas chromatography/mass spectrometry, have been found to have well distributed melting points from <0 °C to >250 °C. Out of 8.94 g/kg OC content, a significant proportion (0.376 g) was an unresolved compound mixture. However, information pertaining to the direct melting/volatilization points of many compounds in that list was not available in our search. And though the disappearance of particles or shrinking of particle diameters at heating temperatures up to 250 °C should be linked with the evaporation of OC contents (even though the sample stream in our heater design represents a kinetic, not thermodynamic equilibrium), candidate compounds are largely absent from the compounds, as implied by the lack of information available pertaining to their evaporation points for most the heating temperature ranges (e.g., no compound between 20 °C and 50 °C, only 1 compound between 50 °C and 100 °C, and no compound between 100 °C and 200 °C). Such voids could be due to OC compounds with little/no information on evaporation points and/or from the unresolved complex mixture; it is expected that further research should reinforce the characterization of such compounds as well as identify the unresolved compound mixtures. In

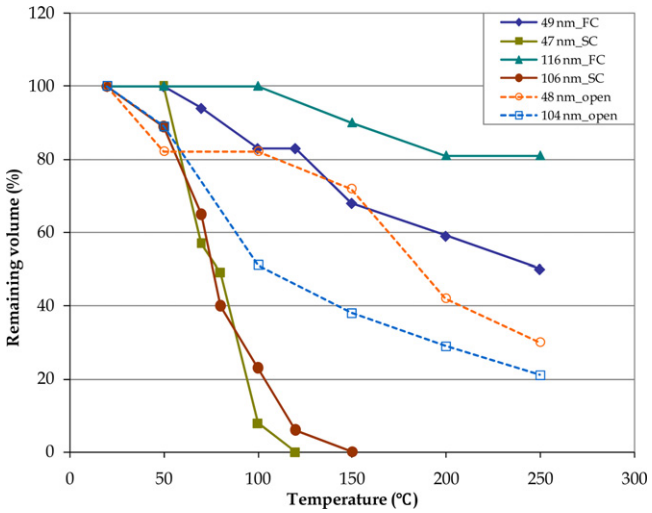

Fig. 6. Average volatility of particles from rice straw burning.

the mean time, the high temperature oxidation of OC compounds and resultant release of CO_2 is seen to lead to a decrease in diameter, rather than simple volatilization upon heating. These contributions assist in providing a more comprehensive understanding of the particles emitted from rice straw combustion.

Fig. 6 summarizes the average volatility of rice straw combustion-emitted ultrafine particles under all burning conditions. The smoldering combustion particles were completely volatilized at 100–150 °C, indicating the absence of a non-volatile core (mostly comprised of BC), which is a remarkable property observed in contrast to the other two combustion conditions. The complete volatilization of smoldering combustion-emitted particles compared to the least volatility of flaming combustion particles indicates the much higher volatile-OC content of the smoldering particles. Open burning and the flaming combustion both resulted in particles containing non-volatile cores comprised of BC and/or non-volatile OC plus other macro-/micro-nutrient elements that exist in plant tissues. This also suggests that there is internal mixing of OC and BC (BC being the usual product in the firing/flaming condition, whereas OC is the volatilized fraction within 250 °C heating).

Zhang et al. [16] reported that the averaged OC in $PM_{2.5}$ from flaming and smoldering combustion of cereal straw (including rice straw) was 54.6 ± 6%, and that EC was much lower. The EC content was reported to be higher in flaming combustion (5.8–11.6%) than in smoldering combustion (4.7–5.3%), though it does not vary substantially. Despite the limitation of our study being size-selected and non-representative of all $PM_{2.5}$, our results suggest that there is significant variation in the EC contents of rice straw, as volatility characteristics indicate there is no non-volatile core in the smoldering combustion particles.

The volatility of the particles emitted from open burning of rice straw is intermediate between flaming and smoldering. The volatile volume per degree Celsius heating temperature for open burning particles also has intermediate values between the flaming and smoldering slopes for rice straw. This suggests an intermediate and arbitrary ranking of the open burning process between the flaming and smoldering processes. Moreover, in Fig. 6 the data trend for 48 nm particles in open burning tends to resemble that for the flaming condition, whereas the trend for 104 nm particles in open burning 104 nm tends to resemble that for the smoldering condition. Note that the openness of the burning location as well as wind flow results in air renewal and would replenish the oxygen supply, thereby shifting the open burning condition toward a prolonged resemblance to flaming combustion. Conversely, the still air condition (available oxygen being used up) and overload of fuel would push the open burning condition more toward smoldering a short time after the initiation of burning. Such positioning of open burning between the conditions for flaming and smoldering combustions has an extremely important implication for the management of open field biomass burning, including both climate forcing properties [3,8,28–32], and public health risks [33–36].

3.3. *Supporting Information* from TEM/EDS particle analyses

Fig. SI-2 (flaming, smoldering, open burning), Fig. SI-3 (flaming, smoldering), and Fig. SI-4 (flaming, smoldering) present the TEM/EDS data for rice straw, oak, and pine combustion emitted particles, respectively (Supporting Information). Approximately 50 ultrafine particles in sizes of 50–200 nm were examined at each condition. In the morphological analyses of these particles it can be seen that in rice straw burning, flaming combustion (Fig. SI-2A) results in open structures, whereas smoldering combustion (Fig. SI-2B) produces closed structures. The particle structure in open burning (Fig. SI-2C) is similar to that in between the flaming (open structure) and smoldering (closed structure) particle structures. This finding further supports the arbitrary intermediate positioning of the open burning condition between flaming and smoldering, which affects particle morphology during formation. In the case of wood combustion particles, pine (softwood) flaming (Fig. SI-4A) and smoldering (Fig. SI-4B) particle structures resemble those of rice straw combustion particles; however, oak (hardwood) flaming (Fig. SI-3A) and smoldering (Fig. SI-3B) both exhibit structures at an intermediate stage between open and closed types (resembling rice straw open burning, Fig. SI-2C). Nevertheless, although we observed structural differences among the particles, identifying the existence of volatile organic compounds due to their possible evaporation in a high vacuum environment remains difficult in TEM.

In a compositional comparison from EDS data it can be seen that other than C and O as major constituents, particles from all three biomasses for all burning conditions commonly contain Si and K as additional components. In addition, smoldering combustion particles from rice straw also contains S and Al, while S and Cl are present in oak flaming combustion particles, and Cl in pine flaming combustion particles. Therefore, the presence of C and O as major constituents indicates the carbonaceous nature of all these particles, while the existence of Si, K, S, Al, and Cl suggests the presence of inorganic species from macro- and micro-nutrients in the plant biomasses. Those inorganic species can affect hygroscopic properties of particles burned from biomasses [44].

4. Conclusions

A clear distinction was observed among the burning conditions, which can be summarized as follows: (i) >200 °C flue gas temperature in flaming combustion, and <200 °C in smoldering combustion, and (ii) a smoldering to flaming with CO emission ratio of >1, which forms a better parameter than the CO/CO_2 ratio. These distinctions were observed in all combustion conditions for all three fuels used in this study. Combustion of wood more vulnerable to burning (softwood) resulted in larger mode diameters than from wood less vulnerable to burning (hardwood). Differential size distribution characteristics for the biomasses are explained with regard to the basic natures of the particles, along with the observed volatility and mixing states. Ultrafine particle emitted from rice straw during smoldering combustion were completely volatilized by heating them to 150 °C, whereas the majority of the flaming combustion-emitted particles retained a non-volatile core until 250 °C. Rice straw open burning particles exhibited a volatilization

behavior similar to that between flaming and smoldering combustion, indicating that the condition of open burning could be ranked at some arbitrary position between them. The oak and pine smoldering combustion-emitted particles were almost completely volatilized by 250 °C, while the majority of volume remained for the flaming combustion condition. In addition, internal mixing states were observed in all three biomasses for all burning conditions, though external mixing states were only observed for rice straw combustion-emitted particles. While the flaming combustion and open burning results imply there is internal mixing of OC and BC, smoldering combustion in rice straw produced ultrafine particles devoid of BC. Such different mixing states, sizes, and volatility of particles depending on biomass fuel characteristics and the combustion condition are of great importance for their alternation of the single scattering albedo and radiative forcing, and roles in cloud formation.

Acknowledgments

The research described in this paper was supported by National Research Foundation of Korea (NRF) grant funded by the Korea government (MEST) (No. 2011-0015548) and the Basic Research Project through a grant provided by the Gwangju Institute of Science and Technology (GIST), Rep. of Korea.

Appendix A. Supplementary data

Supplementary data associated with this article can be found, in the online version, at doi:10.1016/j.jhazmat.2011.12.061.

References

[1] IPCC, in: R.K. Pachauri, A. Reisinger (Eds.), Climate Change 2007: Synthesis Report. Contribution of Working Groups I, II and III to the Fourth Assessment Report of the Intergovernmental Panel on Climate Change, IPCC, Geneva, Switzerland, 2007.
[2] J.A. Bernstein, N. Alexis, C. Barnes, I.L. Bernstein, J.A. Bernstein, A. Nel, D. Peden, D. Diaz-Sanchez, S.M. Tarlo, P.B. Williams, Health effects of air pollution, J. Allergy Clin. Immun. 114 (2004) 1116–1123.
[3] U. Pöschl, Atmospheric aerosols: composition, transformation, climate and health effects, Angew. Chem. Int. Ed. 44 (2005) 7520–7540.
[4] C. Alves, A. Vicente, T. Nunes, C. Gonçalves, A.P. Fernandes, F. Mirante, L. Tarelho, A. Sanchez de la Campa, X. Querol, A. Caseiro, C. Monteiro, M. Evtyugina, C. Pio, Summer 2009 wildfires in Portugal: emission of trace gases and aerosol composition, Atmos. Environ. 45 (2011) 641–649.
[5] P.M. Fine, G.R. Cass, B.R.T. Simoneit, Chemical characterization of fine particle emissions from fireplace combustion of woods grown in the Midwestern and western United States, Environ. Eng. Sci. 21 (2004) 387–409.
[6] C. Gonçalves, C. Alves, A.P. Fernandes, C. Monteiro, L. Tarelho, M. Evtyugina, C. Pio, Organic compounds in $PM_{2.5}$ emitted from fireplace and woodstove combustion of typical Portuguese wood species, Atmos. Environ. 45 (2011) 4533–4545.
[7] C. Schmidl, I.L. Marr, A. Caseiro, P. Kotianová, A. Berner, H. Bauer, A. Kasper Giebl, H. Puxbaum, Chemical characterisation of fine particle emissions from woodstove combustion of common woods growing in mid-European Alpine regions, Atmos. Environ. 42 (2008) 126–141.
[8] S. Menon, Current uncertainties in assessing aerosol effects on climate, Annu. Rev. Environ. Resour. (2004) 1–30.
[9] H.A. Gray, G.R. Cass, J.J. Huntzicker, E.K. Heyerdahl, J.A. Rau, Characteristics of atmospheric organic and elemental carbon particle concentrations in Los Angeles, Environ. Sci. Technol. 20 (1986) 580–589.
[10] K. Cheung, N. Daher, W. Kam, M.M. Shafer, Z. Ning, J.J. Schauer, C. Sioutas, Spatial and temporal variation of chemical composition and mass closure of ambient coarse particulate matter (PM10-2.5) in the Los Angeles area, Atmos. Environ. 45 (2011) 2651–2662.
[11] B. Gomiscek, A. Frank, H. Puxbaum, S. Stopper, O. Preining, H. Hauck, Case study analysis of PM burden at an urban and a rural site during the AUPHEP project, Atmos. Environ. 38 (2004) 3935–3948.
[12] D.C. Snyder, A.P. Rutter, C. Worley, M. Olson, A. Plourde, R.C. Bader, T. Dallmann, J.J. Schauer, Spatial variability of carbonaceous aerosols and associated source tracers in two cites in the Midwestern United States, Atmos. Environ. 44 (2010) 1597–1608.
[13] P.M. Fine, G.R. Cass, B.R.T. Simoneit, Chemical characterization of fine particle emissions from the fireplace combustion of woods grown in the Southern United States, Environ. Sci. Technol. 36 (2002) 1442–1451.
[14] M.D. Hays, P.M. Fine, C.D. Geron, M.J. Kleeman, B.K. Gullett, Open burning of agricultural biomass: physical and chemical properties of particle-phase emissions, Atmos. Environ. 39 (2005) 6747–6764.
[15] M.J. Kleeman, J.J. Schauer, G.R. Cass, Size and composition distribution of fine particulate matter emitted from wood burning, meat charbroiling, and cigarettes, Environ. Sci. Technol. 33 (1999) 3516–3523.
[16] Y.x. Zhang, M. Shao, Y.h. Zhang, L.m. Zeng, L.y. He, B. Zhu, Y.j. Wei, X.l. Zhu, Source profiles of particulate organic matters emitted from cereal straw burnings, J. Environ. Sci. 19 (2007) 167–175.
[17] R.K. Chakrabarty, H. Moosmüller, L.W.A. Chen, K. Lewis, W.P. Arnott, C. Mazzoleni, M.K. Dubey, C.E. Wold, W.M. Hao, S.M. Kreidenweis, Brown carbon in tar balls from smoldering biomass combustion, Atmos. Chem. Phys. 10 (2010) 6363–6370.
[18] J.A. Rau, Composition and size distribution of residential wood smoke particles, Aerosol Sci. Technol. 10 (1989) 181–192.
[19] J. Tissari, K. Hytonen, J. Lyyranen, J. Jokiniemi, A novel field measurement method for determining fine particle and gas emissions from residential wood combustion, Atmos. Environ. 41 (2007) 8330–8344.
[20] J. Tissari, J. Lyyranen, K. Hytonen, O. Sippula, U. Tapper, A. Frey, K. Saarnio, A.S. Pennanen, R. Hillamo, R.O. Salonen, M.R. Hirvonen, J. Jokiniemi, Fine particle and gaseous emissions from normal and smouldering wood combustion in a conventional masonry heater, Atmos. Environ. 42 (2008) 7862–7873.
[21] A.Y.P. Wardoyo, L. Morawska, Z.D. Ristovski, J. Marsh, Quantification of particle number and mass emission factors from combustion of Queensland trees, Environ. Sci. Technol. 40 (2006) 5696–5703.
[22] R.K. Chakrabarty, H. Moosmüller, M.A. Garro, W.P. Arnott, J. Walker, R.A. Susott, R.E. Babbitt, C.E. Wold, E.N. Lincoln, W.M. Hao, Emissions from the laboratory combustion of wildland fuels: particle morphology and size, J. Geophys. Res. 111 (2006) D07204.
[23] L.W.A. Chen, H. Moosmüller, W.P. Arnott, J.C. Chow, J.G. Watson, R.A. Susott, R.E. Babbitt, C.E. Wold, E.N. Lincoln, W.M. Hao, Emissions from laboratory combustion of wildland fuels: emission factors and source profiles, Environ. Sci. Technol. 41 (2007) 4317–4325.
[24] G.R. McMeeking, S.M. Kreidenweis, S. Baker, C.M. Carrico, J.C. Chow, J.L. Collett, W.M. Hao Jr., A.S. Holden, T.W. Kirchstetter, W.C. Malm, H. Moosmüller, A.P. Sullivan, C.E. Wold, Emissions of trace gases and aerosols during the open combustion of biomass in the laboratory, J. Geophys. Res. 114 (2009) D19210.
[25] M.D. Petters, C.M. Carrico, S.M. Kreidenweis, A.J. Prenni, P.J. DeMott, J.L. Collett Jr., H. Moosmüller, Cloud condensation nucleation activity of biomass burning aerosol, J. Geophys. Res. 114 (2009) D22205.
[26] J. Ferin, G. Oberdörster, D. Penney, S. Soderholm, R. Gelein, H. Piper, Increased pulmonary toxicity of ultrafine particles? I. Particle clearance, translocation, morphology, J. Aerosol Sci. 21 (1990) 381–384.
[27] G. Oberdorster, Significance of particle parameters in the evaluation of exposure-dose–response relationships of inhaled particles, CRC (1996) 73.
[28] V. Ramanathan, P.J. Crutzen, J.T. Kiehl, D. Rosenfeld, Aerosols, climate, and the hydrological cycle, Science 294 (2001) 2119–2124.
[29] A. Gelencser, Carbonaceous Aerosol, Springer, Dordrecht, 2004.
[30] P. Forster, V. Ramaswamy, P. Artaxo, T. Berntsen, R. Betts, D.W. Fahey, J. Haywood, J. Lean, D.C. Lowe, G. Myhre, J. Nganga, R. Prinn, G. Raga, M. Schulz, R. Van Dorland, Changes in atmospheric constituents and in radiative forcing, in: S. Solomon, D. Qin, M. Manning, Z. Chen, M. Marquis, K.B. Averyt, M. Tignor, H.L. Miller (Eds.), Climate Change 2007: The Physical Science Basis. Contribution of Working Group I to the Fourth Assessment Report of the Intergovernmental Panel on Climate Change, 2007.
[31] T. Novakov, V. Ramanathan, J.E. Hansen, T.W. Kirchstetter, M. Sato, J.E. Sinton, J.A. Sathaye, Large historical changes of fossil-fuel black carbon aerosols, Geophys. Res. Lett. 30 (2003) 1324–1327.
[32] M. Sato, J. Hansen, D. Koch, A. Lacis, R. Ruedy, O. Dubovik, B. Holben, M. Chin, T. Novakov, Global atmospheric black carbon inferred from AERONET, Proc. Natl. Acad. Sci. U.S.A. 100 (2003) 6319–6324.
[33] L.M. McKenzie, W.M. Hao, G.N. Richards, D.E. Ward, Measurement and modeling of air toxins from smoldering combustion of biomass, Environ. Sci. Technol. 29 (1995) 2047–2054.
[34] T. Korenaga, X. Liu, Z. Huang, The influence of moisture content on polycyclic aromatic hydrocarbons emission during rice straw burning, Chemosphere Global Change Sci. 3 (2001) 117–122.
[35] B. Gullett, A. Touati, PCDD/F emissions from burning wheat and rice field residue, Atmos. Environ. 37 (2003) 4893–4899.
[36] L.-F. Lin, W.-J. Lee, H.-W. Li, M.-S. Wang, G.-P. Chang-Chien, Characterization and inventory of PCDD/F emissions from coal-fired power plants and other sources in Taiwan, Chemosphere 68 (2007) 1642–1649.
[37] K. Park, J.S. Kim, H.P. Seung, Measurements of hygroscopicity and volatility of atmospheric ultrafine particles during ultrafine particle formation events at urban, industrial, and coastal sites, Environ. Sci. Technol. 43 (2009) 6710–6716.
[38] L.M. Hildemann, G.R. Cass, G.R. Markowski, A dilution stack sampler for collection of organic aerosol emissions: design, characterization and field tests, Aerosol Sci. Technol. 10 (1989) 193–204.
[39] A.L. Robinson, N.M. Donahue, M.K. Shrivastava, E.A. Weitkamp, A.M. Sage, A.P. Grieshop, T.E. Lane, J.R. Pierce, S.N. Pandis, Rethinking organic aerosols: semivolatile emissions and photochemical aging, Science 315 (2007) 1259.
[40] R. Saleh, A. Shihadeh, A. Khlystov, On transport phenomena and equilibration time scales in thermodenuders, Atmos. Meas. Tech. 4 (2011) 571–581.
[41] C. Neusüß, E. Brüeggemann, T. Gnauk, H. Wex, H. Herrmann, A. Wiedensohler, Chemical composition and mass closure of the size-segregated atmospheric aerosol in Falkenberg during LACE, J. Aerosol Sci. 30 (1999) S913–S914.

[42] M.J. Kleeman, M.A. Robert, S.G. Riddle, P.M. Fine, M.D. Hays, J.J. Schauer, M.P. Hannigan, Size distribution of trace organic species emitted from biomass combustion and meat charbroiling, Atmos. Environ. 42 (2008) 3059–3075.
[43] E.M. Lipsky, A.L. Robinson, Effects of dilution on fine particle mass and partitioning of semivolatile organics in diesel exhaust and wood smoke, Environ. Sci. Technol. 40 (2006) 155–162.
[44] C.M. Carrico, M.D. Petters, S.M. Kreidenweis, A.P. Sullivan, G.R. McMeeking, E.J.T. Levin, G. Engling, W.C. Malm, J.L. Collett Jr., Water uptake and chemical composition of fresh aerosols generated in open burning of biomass, Atmos. Chem. Phys. 10 (2010) 5165–5178.